THE SYNTHESIS OF THE SOUND FIELD EXCITED BY A RIGID BODY OF ARBITRARY SHAPE IN AIR WITH AN ARBITRARY DISTRIBUTION OF NORMAL VELOCITIES BY SPHERICAL SOUND FIELDS

L. Cremer

Technical University, Berlin

To introduce my nomenclature and symbols I will start with the problem of the simplest idealised sound source, a sphere in infinite, empty space. For this problem, the sound pressure outside the sphere can always be described in terms of a double sum of products of three functions. The first function, R say, depends only on the radial distance r from the sphere's centre and the acoustic wavenumber k, in the combination (kr). The second function, Θ say, depends on the angle of declination θ, and the third function depends on the azimuthal angle ϕ. This last may be written as

$$\Phi_n(\varphi) = \cos\left(n(\varphi - \varphi_n)\right) . \qquad (1)$$

where n denotes the number of node-lines in the ϕ-direction. The function $\Theta(\theta)$ is characterised by values of two parameters: n, and the number (m say) of node-lines in the θ-direction, while the radial function R changes with m only. These products, which describe what may be called the m,n-modes making up the total sound field I call "spherical sound fields".

Summing over them, we can express the actual sound pressure in the form

$$\underline{p}(r,\vartheta,\varphi) = \sum_{m=0}^{\infty} \sum_{n=0}^{m} \underline{p}_{mn}\left[\underline{R}_m(kr)\,\Theta_{mn}(\vartheta)\,\Phi_n(\varphi)\right] \Big/ \underline{R}_m(kh) \quad . \qquad (2)$$

Since the modal terms are dimensionless, their complex (and therefore underlined) amplitudes are pressures as well. It is sensible to normalise them by dividing each term by $\underline{R}_m(kh)$, so that they all describe pressures at the same value r = h, which we may take to be the radius of the exciting sphere.

The dimensionless number kh characterises a similarity group. In aerodynamics we are accustomed to characterise similar fields by such similarity numbers — for example the Reynolds number, which when small leads us to expect laminar flow, and when large, turbulent flow. In the same sense here, small kh implies quasi-stationary, incompressible fields near the surface of the sphere, while large kh implies waves of radiating character while still close to the sphere. To emphasise these general relationships, which hold also for sources of any shape, allow me to give kh a special name. Since this similarity appeared first in the wave equation for pure tones, which is often called the Helmholtz equation, I call the ratio of a characteristic length to the wavelength in any sound field a "Helmholtz number" /1/. In this case I will apply that term to the number kh, by regarding the perimeter of the radiating sphere as a suitable characteristic length.

SOUND FIELD SYNTHESIS

If we set r = h in (2), we obtain

$$\underline{p}(h,\vartheta,\varphi) = \sum\sum \underline{P}_{mn}\,\Theta_{mn}(\vartheta)\,\Phi_n(\varphi) \;. \tag{2a}$$

Since r is constant, only the functions Θ_{mn} and Φ_n appear here. These are both purely real functions, although their amplitudes will in general be complex. Lord Rayleigh /2/ called them "spherical harmonics", and therefore designated their products by S_{mn}:

$$S_{mn} = \Theta_{mn}(\vartheta)\;\Phi_n(\varphi) \;. \tag{3}$$

They share with other eigenfunctions the extraordinary property of orthogonality:

$$\int_S S_{mn}\,S_{m'n'}\,dS = 0 \quad ; \quad m,n \neq m',n' \;. \tag{4}$$

This property makes the analysis of a given distribution of a field quantity into its spherical harmonic components very easy, since each coefficient may be calculated independently. Multiplying both sides of equation (2a) by $S_{m'n'}(\theta,\phi)$ and integrating over the whole sphere leaves just one non-zero term from the double sum on the right-hand side, so that the amplitude $\underline{P}_{m'n'}$ may be deduced immediately:

$$\int_S \underline{p}(\vartheta,\varphi)\,S_{m'n'}(\vartheta,\varphi)\,dS = \underline{P}_{m'n'}\int_S S^2_{m'n'}(\vartheta,\varphi)\,dS \;. \tag{5}$$

We must now decide which field quantity we wish to regard as given. If we were dealing with the problem of a very thin spherical shell in water, perhaps pressure would be the appropriate quantity. However, I emphasised in the title that I am concerned here with rigid bodies in air. For such bodies, the impedance of the body will be large in comparison with that of the surrounding air, so that it is appropriate to regard the normal velocity as being given. We may readily relate the pressure terms appearing in (2) to the corresponding terms in radial velocity:

$$\underline{P}_{mn} = -j\rho c\,\underline{v}_{rmn}\,\underline{R}_m(kh)/\underline{R}'_m(kh) \tag{6}$$

and we can thus analyse $\underline{v}_r(\theta,\phi)$ into spherical harmonics.

Our primary interest is in the sound pressure distribution at large distances, say over a distant sphere of radius e. An important property of all the functions $\underline{R}_m$ makes the choice of an appropriate value of e simple. $\underline{R}_m$ is so defined that each $\underline{R}_m$ tends towards a pure spherical wave when ke becomes large:

$$(kr)^2 >> 1 \quad ; \quad \underline{R}_m \longrightarrow \frac{e^{-jkr}}{(kr)} \;. \tag{7}$$

Only in this far field is it sensible to define — or measure — a directional characteristic (which could be expressed in its spherical harmonics). We would naturally express the amplitudes of modes by partial pressures on that sphere r = e:

$$\underline{p}(e,\vartheta,\varphi) = \sum\sum \underline{P}_{emn}\,S_{mn}(\vartheta,\varphi) \;. \tag{8}$$

SOUND FIELD SYNTHESIS

From the relations given above, we could either calculate the directional characteristic for a given radial velocity distribution, or, just as easily, the converse. However, in practice there is a great difference between these two. The larger the value of m compared to the Helmholtz number, the more rapidly do the functions $\underline{R}_m$ and $\underline{R}'_m$ increase towards the source. Thus a corrugated distribution of $\underline{v}_r$ on the source sphere may appear hardly at all in the directional characteristic since the effect of the higher m values is relatively attenuated as we move away from the source. This attenuation could be reliably predicted without major problems of ill-conditioning. However, to go in the opposite direction and try to deduce conditions at the source from the far-field pattern could involve serious problems of this type, since very small components in the directional characteristic would have to multiplied by very large factors to find the distribution of $\underline{v}_r$. Fortunately, we are seldom required to infer behaviour at source from far-field radiation patterns, whereas it is quite frequently of interest to replace the laborious measurement of a directional characteristic by the sensing of velocities on the source and the calculation of the directional characteristic. For example, with large machinery there is usually no possibility of measuring at sufficiently large distances and in an anechoic room.

Here we can best make the jump to consider sources of arbitrary shape. For any finite source, provided we are sufficiently far away from it, the field may be decomposed into a universal function of distance as in (7), multiplied by a function of θ and ϕ which can be analysed into spherical harmonics. In this case, however, not only must r be large in comparison with wavelength λ, giving what is usually called a "far" (in contrast to a "near") field, but it must also satisfy

$$r \gg b_{max} \qquad (9)$$

where b_{max} is the largest dimension of the source in any direction. In my "Physics of the violin" /3/ I called this a "distant" field, in contrast to the "neighbouring" field, which extends from the source to approximately $r=5b_{max}$. This neighbouring field could also be a near field if the Helmholtz number is small, but if the Helmholtz number is large it may consist largely of far field. On the other hand, if the neighbouring field is an incompressible one, then that quality may persist for some way into the distant field. This possibility results in the well-known fact that a concentrated volume flux of any kind tends towards a spherically-symmetric distributed flux before this in turn produces a zero-order spherical wave. If the compressible (far) field starts within the neighbouring field, the eventual spherical wave will have more spherical-harmonic components.

Lord Rayleigh has discussed this problem /2/, noting among other things the fact that, on grounds of symmetry, the sound field produced by any rotationally and equatorial symmetric vibrating body (in the far distant field) will consist only of Θ_m-functions of even order if the motion is symmetric with respect to the equator, or only of odd orders if the two halves vibrate in opposite phases. Rayleigh was not able to give rules to determine the amplitudes in all cases, and he was not concerned with the problem of extending the synthesis of spherical fields to the whole space outside the source.

SOUND FIELD SYNTHESIS

Since the same directional characteristic can be produced by sources of different shapes and appropriately different velocity distributions, it is possible to compare each source with a reference sphere of radius h which would produce the same characteristic. In this spirit, Backhaus /4/ and more recently Weinreich /5/ have compared a body of such a non-spherical shape as a violin with a monopole, a dipole etc. I prefer to compare them with reference spheres producing fields of order 0,1,2... Figure 1 shows the directional characteristics of a violin at two different frequencies, in the plane of the bridge, as measured by Meinel /6/. The dashed line corresponds to the lowest body resonance, which appeared at a frequency of 517 Hz. This corresponds to a wavelength in air of 66 cm. The maximum width of the violin in the cross-direction is about 20 cm, and the minimum is about 12 cm. These values are not so small compared with the wavelength as to make a zero-order characteristic inevitable, but in fact the deviation from a circle is astonishingly small. This contrasts with the solid line, corresponding to the the f-hole or air resonance at the lower frequency of 290 Hz, which looks more like a superposition of a zero and a first order field.

So I felt confronted by the question /7/: for a violin, or indeed for any rigid body of arbitrary shape, does there exist a distribution of normal velocity, which we might denote $\underline{V}(\theta,\phi)$, which produces in the surrounding air a spherical wave field of the order m,n right from the surface of the body? The answer was "yes", and the condition for the $\underline{V}$-distribution was so simple that I was at first in serious doubt as to whether it was really sufficient. $\underline{V}$ is simply set equal to the velocity distribution corresponding to a spherical sound field of order m,n produced by a sphere contained within the body of interest. This boundary condition uniquely determines a forced motion of the air, which has the same pressures and tangential velocity components as the reference field. The tangential components meet no constraint, and on account of the impedance mismatch mentioned above, the rigid source can easily provide these pressures.

Let us look for the most simple example of a non-spherical rigid body. We will naturally choose one with rotational symmetry and equatorial mirror-symmetry. By cutting a sphere of radius a with two parallel planes a distance h either side of the equator we obtain a family of bodies which includes the sphere in the limiting case $h \rightarrow a$. In Fig. 2 the ratio h/a is chosen to be 1/4. We can take a reference sphere which touches the two planes at its poles. We start with the zero-order spherical field, shown in Fig. 2a. For low Helmholtz number, the normal velocity across the top plane decreases like $\cos^3\theta$, and the back plane has a mirror-image distribution. Around the curved sides, the normal velocity is small but constant. Although the violin never vibrates with a "bell-shaped" velocity distribution quite like this, it does execute breathing motions which are qualitatively similar, resulting from the lever action of the bridge and the asymmetric constraint of the soundpost. This results in radiation at the lowest body resonance which approximates a zero-order field, as we have seen.

Figure 2b shows, as the dashed line, the corresponding $\underline{V}$-distribution for a first-order field. Its dependence on θ is a little more complicated, since the tangential components of the spherical field now contribute. However, the shape is still bell-like, the chief difference from the zero-order case being the sign change between top and back plates. If we were to superimpose both $\underline{V}$-distributions with equal amplitudes, we would approximate a source in which high surface velocities are only found near the centre of the top plate, the back plate vibrating little. This corresponds qualitatively to the motion at the air resonance of a violin, with air flow in and out through the f-holes. It thus explains qualitatively the directional characteristic of this resonance seen in Fig. 1, which consists largely of a superposition of zero-order and first-order fields. These examples show how fruitful spherical-field synthesis can be, even for purely qualitative discussions. Our example series is completed, in Fig. 2c, with the $\underline{V}$-distribution for a first-order field in the transverse direction, just to demonstrate that no difficulties arise in the construction of modes in which n does not vanish.

Our aim is to develop a quantitative method for analysing arbitrary $\underline{V}$-distributions at the surface of an arbitrary source body in terms of spherical-field components according to a sum of the type

$$\underline{V}(\vartheta,\varphi) = \sum\sum \underline{V}_{mn}\,\underline{Q}_{mn}(\vartheta,\varphi) \;. \qquad (10)$$

Here we have introduced the dimensionless distribution functions $\underline{Q}$, with maximum values of unity since the reference sphere is inscribed within the body, which create spherical-harmonic fields from an arbitrary source body shape. We need only consider the zero-order field to see immediately that $\underline{Q}_0$ depends on frequency and must therefore in general be complex. At large Helmholtz number (which we take to be kh, where h is the radius of the reference sphere) the radial velocity decreases like 1/r and contains a phase delay.

As a preparatory study, however, we may restrict attention to low Helmholtz numbers, when all the $\underline{Q}_{mn}$ terms represent incompressible velocity fields and are thus real, like the spherical harmonics. We must note an essential difference, though: these functions, although real, are not in general orthogonal. Thus the integral corresponding to (5) will in general produce on the right-hand side a sum of terms containing all $\underline{V}_{mn}$:

$$\int_S \underline{V}(\vartheta,\varphi)\,\underline{Q}_{m'n'}\,dS = \sum\sum \underline{V}_{mn}\int \underline{Q}_{mn}\underline{Q}_{m'n'}\,dS \;. \qquad (11)$$

If we truncate this sum by estimating a likely number M of necessary spherical fields, we obtain M equations for M unknowns, so that there will in general be a unique solution. We then need to check convergence by repeating the calculation with increased M. In contrast to the spherical harmonics, where the amplitudes already calculated are unchanged by such an increase, we here have to allow for all the $\underline{V}_{mn}$ to change. Fortunately, this influence seems empirically to be restricted to the neighbours of the new term, but this is not guaranteed.

SOUND FIELD SYNTHESIS

It would be possible to extend the approach of equation (11), i.e. this system of M equations, to complex functions $\underline{Q}$. The approach I prefer, from my paper in Acustica **55**, takes its cue from successful experience with problems involving forced vibrations in tubes with difficult boundary conditions /1/. We first multiply $\underline{V}(\theta,\phi)$ on the left-hand side of (10) by the complex conjugate of the function $\underline{\Pi}_{mn}(\theta,\phi)$ occurring in the analogous decomposition of the pressure distribution into spherical waves:

$$\underline{p}(r_s,\vartheta,\varphi) = \sum\sum \rho c \underline{V}_{mn} \underline{\Pi}_{mn}(\vartheta,\varphi) \, , \qquad (12)$$

which can also be derived from the corresponding field excited by the reference sphere. We thus write

$$\int_S \underline{V}(\vartheta,\varphi)\underline{\Pi}^*_{m'n'}\, dS = \sum\sum \underline{V}_{mn} \int \underline{Q}_{mn}\underline{\Pi}^*_{m'n'}\, dS \, . \qquad (13)$$

This procedure has the advantage that the coefficients $\underline{V}_{mn}$ appearing on the right-hand side can be interpreted as partial powers /8/. The real parts of the diagonal coefficients (in the sense that m = m', n = n') in the right-hand side matrix represent the radiated powers P_{mn} of the m,n mode:

$$P_{mn} = \frac{1}{2}\rho c\, V^2_{mn}\, Re\left\{ \int_S \underline{Q}_{mn}\underline{\Pi}^*_{mn}\, dS\right\} \, . \qquad (14)$$

When the Helmholtz number is small, pressure is almost in quadrature with velocity so that these terms are small. Then, the $\underline{V}_{mn}$ may be calculated to a reasonable approximation by ignoring radiation, although radiation obviously governs the directional characteristic and is our main topic. Since the radiated power for each mode m,n is that radiated by the reference sphere, it is more easily calculated by multiplying V^2_{mn} found in this way by the well-known radiation resistance for the corresponding mode.

The imaginary part of a given diagonal coefficient corresponds to the time derivative of the kinetic energy due to the incompressible part of the velocity field: normalising again to $1/2\, \rho c V^2_{mn}$, we have

$$-2\omega W_{mn} = \frac{1}{2}\rho c\, V^2_{mn}\, Im\left\{ \int_S \underline{Q}_{mn}\underline{\Pi}^*_{mn}\, dS\right\} \qquad (15)$$

Thus for both real and imaginary parts of the diagonal coefficients, we have available a check by a second method. The same is true of the imaginary parts of the coupling coefficients. If we take the sum of a pair of coefficients symmetrically-disposed about the main diagonal of the matrix, it can be expressed as the time derivative of the "mutual" kinetic energy:

$$\frac{\rho c}{2}\underline{V}_{mn}\underline{V}^*_{m'n'} Im\left\{\int_S \underline{Q}_{mn}\underline{\Pi}^*_{m'n'}\, dS\right\} + \frac{\rho c}{2}\underline{V}^*_{mn}\underline{V}_{m'n'} Im\left\{\int_S \underline{Q}_{m'n'}\underline{\Pi}^*_{mn}\, dS\right\} = -2\omega \left|\underline{W}_{mnm'n'}\right| \qquad (16)$$

SOUND FIELD SYNTHESIS

The term "mutual energy" was first introduced by Heaviside /9/. If two field quantities are superimposed, for example velocities $v_m + v_n$, the square of the resulting field consists of the sum $v_m^2 + v_n^2$, plus the mutual term $2v_mv_n$. If the terms v_m^2 and v_n^2 satisfy separate power-balance conditions, then the mutual terms must have their own power balance. Heaviside studied these balances back in 1892, and I became acquainted with his results through Karl Willy Wagner /10/. Heaviside considered a system having a finite number of degrees of freedom, acted on by two superimposed sets of forces: a set $\underline{F}_{ak}$ which produce velocities $\underline{v}_{ak}$ at masses m_k, and a set $\underline{F}_{bk}$ producing corresponding velocities $\underline{v}_{bk}$. The mutual power can then be split in two parts:

$$\sum_k \underline{F}_{ak}\underline{v}_{bk} + \sum_k \underline{F}_{bk}\underline{v}_{ak} \quad .$$

The studies of Heaviside, and later Wagner, show that for a system consisting entirely of lumped masses, springs and linear viscous resistances, the two terms are equal. For the special case in which we take only one force of each set to be non-zero, this result becomes the well-known law of reciprocity. The Heaviside-Wagner "law of mutual powers" can be regarded as a generalisation, and it can also be applied in an integral form to continuous systems such as the problem we are considering. For our case, it results in the statement that the two terms on the left-hand side of (16) are equal. Since the two quantities $\underline{v}_{mn}\underline{v}^*_{m'n'}$ and $\underline{v}^*_{mn}\underline{v}_{m'n'}$ are complex conjugates, we can conclude that the imaginary parts of the symmetric coefficients in our matrix must be equal:

$$\mathrm{Im}\left\{ \int_S \underline{Q}_{mn}\underline{\Pi}^*_{m'n'}\,dS \right\} = \mathrm{Im}\left\{ \int_S \underline{Q}_{m'n'}\underline{\Pi}^*_{mn}\,dS \right\} \quad . \tag{17}$$

I now return to the simple example in Fig. 2, which allows this statement to be checked by a simple analytic calculation. In Table 1, the first column shows values of $\dfrac{\mathrm{Im}\left\{\int_S \underline{Q}_0\underline{\Pi}_2^*dS\right\}}{(-4\pi kh^3)}$ and the second column values of $\dfrac{\mathrm{Im}\left\{\int_S \underline{Q}_2\underline{\Pi}_0^*dS\right\}}{(-4\pi kh^3)}$

Since the integrals over top plate and back plate and over the spherical zone are different, we give their results separately in the first two rows. It is not perhaps surprising, but nevertheless interesting, that only the sum in the third row shows equality. The difference in the contributions of the plates and the zone results physically from the fact that $\underline{Q}_0$ contains only radial velocity components, while $\underline{Q}_2$ contains tangential components as well. These latter cause some tangential power transport. Finally, we should note that these mutual coefficients vanish if h = a, i.e. when the body becomes a complete sphere, since the $\underline{Q}$ and $\underline{\Pi}$ functions then become spherical harmonics. It follows from the integrals in (11) that only the diagonal coefficients remain when the mode distribution functions are orthogonal. Conversely, orthogonality can always be interpreted physically as the vanishing of mutual energies or powers.

SOUND FIELD SYNTHESIS

In any case, to proceed to higher Helmholtz numbers and mode numbers use must be made of a computer. I am grateful to Manfred Heckl for encouraging a visiting Chinese graduate student to undertake the necessary computer work, and I could not have found a better collaborator than Maohui Wang /11/. Table 2 shows some of his results, in the form of the real and imaginary parts of the coefficient matrix for orders 0,2,4 and 6, using as a model equatorially-symmetric excitation of a cylinder of height 2h and diameter 2b, where h/b was chosen to be 1/4, for the rather low Helmholtz number of 0.2. As would be expected, the imaginary parts, representing kinetic energies, are always large compared with the real parts, representing radiated powers. (Note that E-19 means 10^{-19}.) Only the 00-term is comparable to its imaginary partner.

It came as a surprise to me to find non-zero real parts to the coupling coefficients. Since we have no viscous losses in this model, radiation is the only energy-loss mechanism, and this crosses the surface of the source in any direction in the same way that it crosses any sphere in the far distant field. I had thus concluded from the Heaviside-Wagner law of mutual powers that off-diagonal terms would have no real parts. But they appear in the results, and with opposite signs for the corresponding pairs of coefficients. They must thus describe not energy losses, but transfer of power between one mode and another. For a system with lumped elements, this can be achieved by the idealised transformer, a lever. In an aerodynamic continuum, a change in cross-section can work in the same way. Applying the Heaviside analysis to these terms does indeed produce Wang's statement /11/:

$$Re\left\{ \int_S \underline{Q}_{mn} \underline{\Pi}^*_{m'n'} dS \right\} = -Re\left\{ \int_S \underline{Q}_{m'n'} \underline{\Pi}^*_{mn} dS \right\} . \qquad (18)$$

In Table 2 the Helmholtz number of 0.2 is so small that all real components are insignificant compared with the corresponding imaginary ones, so that the result is without practical significance.

Table 3 shows the real and imaginary parts for the same cylinder shape, but with the Helmholtz number increased 16-fold to 3.2. Here the real parts are much bigger, and indeed are larger than the imaginary parts in most cases. Without doubt the calculation has become more difficult at this higher Helmholtz number, but it would be wrong to suppose that this tendency makes the synthesis for very high Helmholtz numbers impossible. If they become sufficiently high that radiating waves start directly from the surface everywhere, we could construct the field according to geometric rules, as Morse and Ingard /12/ have done for the sphere.

Wang's choice for the V(θ) distribution involved no motion of the cylindrical shell, and assumed the function $\cos^2\theta$ over the top and back plates (in the sense of a breathing motion), made to vanish at the circular boundaries. Figure 3 shows progressive stages of the synthesis of this distribution, for the case h = b. In each of the three diagrams, the dashed line shows the assumed V(θ). The solid lines show the sum of calculated terms

SOUND FIELD SYNTHESIS

$\underline{V}_m \underline{Q}_m$ up to $m_{max} = 2, 4$, and 6 respectively, calculated for the case of Helmholtz number 0.2 (since otherwise we would have had to plot real and imaginary parts). It is remarkable how well the assumed shape is fitted with just the zero and second order terms. Adding the term for $m = 4$ makes the fit if anything worse, and adding in $m = 6$ makes it closer again, but scarcely any better than the case with two terms only. This sort of behaviour is to be expected in the absence of orthogonality.

Our main aim is to find the directional characteristic corresponding to a given velocity distribution, so we next investigate how this changes with m_{max}. Figures 4 to 7 each show on the left the shape of the cylinder and assumed velocity distribution, and on the right the wavelength, or a part of one, on the same scale. Below these appear four directional characteristics corresponding to partial sums with increasing numbers of terms. In each case two characteristics are shown, with the lower order dotted and the higher solid, so that the change from one order to the next can be seen easily. The decreasing difference between succeeding pairs shows the convergence of the approximation process. Since the problem has rotational symmetry, it suffices to plot the right half only in each case, while on the left we plot for comparison (as a dashed line) the familiar approximation by a zero-order characteristic with the same total volume flux. In the case of Fig. 4 ($h/b = 1$, $kh = 0.2$) that simple approximation matches our results well and can be regarded as an entirely adequate description. The same holds for Fig. 5 ($h/b = 1/4$, $kh = 0.2$). This shows that an idealised breathing mode of an idealised violin exhibits an ideal zero-order characteristic! Since the situation is qualitatively comparable with the dashed line in Fig. 1, we might perhaps be surprised that the violin does not exhibit an even better approximation to the zero-order characteristic. This arises, no doubt, from the fact that in the real violin the part of the top plate on the narrow side of the sound-post moves in the opposite phase to the rest.

The results for larger Helmholtz number are more interesting. Figure 6 shows results for $h/b = 1$, $kh = 3.2$, and Fig. 7 shows $h/b = 1/4$ with the same Helmholtz number. In both cases the resulting characteristics differ so much from the zero-order contribution that it would have made little sense to supply the corresponding dashed-line comparison on the left-hand side. As soon as the second-order partial is added in, the characteristic becomes quite similar to its final shape. In Fig. 6 this final shape is well approached by adding in the fourth partial, whereas in Fig. 7 the process has not quite converged and the next term, involving the tenth-order partial, would perhaps be desirable.

Shortly after Wang had finished his thesis, in which he also compared calculated characteristics with measured ones, a paper by Akyol /13/ appeared in Acustica, also treating the problem of the sound field of a finite cylinder. He too considered the normal velocity to be the given quantity, and he used a method based on the Helmholtz integral, to obtain an integral equation for the unknown pressure, which he then solved by splitting the cylinder into finite ring-elements. Their number m led to m equations for the m partial amplitudes. The solid line in Fig. 8 shows the pressure calculated in this way, plotted against distance along a surface which runs from the middle of the top plate, parallel to the top, round the corner, and down the side to the middle of the cylindrical shell. He assumed a ratio $h/b = 2$, a Helmholtz number $kh = 2$, and a velocity distribution which was constant over the cylindrical shell and zero over the end-plates. The various marked points were also given in Akyol's paper, following a careful study by him of the existing literature /14/,/15/,/16/,/17/. These points represent studies all by different methods, and all of them different from ours. Wang calculated answers to the same problem by our method with $m_{max} = 14$, and obtained the results plotted as the dashed line on Akyol's diagram. Our results do not differ from the others any more than they differ from each other, and with increased numbers of partial amplitudes they should coincide.

Of the various papers cited above, the most exciting and important for the purposes of comparison with our method is one by Williams, Parke, Moran and Sherman /18/, who also made use of spherical fields. They too regarded normal velocity at the surface for each mode as the self-evident boundary condition, although they were apparently interested in underwater sources. I was very surprised that their method had not found its way into the international handbooks which I had consulted. The reason may have been their modest title, "Acoustic radiation from a finite cylinder", which did not advertise the fact that they were presenting a new general method which could be applied to sources of any shape. Their method differs from ours in one essential respect. Their central equation for the amplitudes of the modes was obtained from an integral of the product of $\underline{V}(\theta)$ and $\underline{\Omega}^*_m$ (in our notation), obtained via the well-known method of minimising the sum of squares of the complex differences between $\underline{V}(\theta)$ and the sum over the series $\underline{V}_m\underline{\Omega}_m(\theta)$.

Their method was actually described in terms of finding the velocity distribution. In Fig. 8, their corresponding pressure distribution (calculated by Wang, again with $m_{max} = 14$) is plotted as a dash-dotted line. Since we do not know the "true" curve, there is no way of telling which of the two methods produces the better fit. However, we can compare the velocity distributions calculated by the two methods with the assumed velocity distribution. This comparison is shown in Fig. 9. We see that over the top plate our method gives lower values, and so comes closer to the assumed value of zero. However, over the cylinder the oscillations around the true constant value have a smaller amplitude as calculated by the method of Williams et al. These oscillations are reminiscent of those in a Fourier analysis of a rectangular pulse, where oscillations appear with about the period of the first neglected overtone. Since here that period corresponds to only about a tenth of the wavelength, the oscillations will cause incompressible near-fields, but virtually no radiation to the far field. Thus for calculating directional characteristics, also done by Wang and shown in Fig. 10, the two methods are scarcely distinguishable.

SOUND FIELD SYNTHESIS

REFERENCES

/1/ Cremer, L. and Muller, H.A.: Principles and Applications of Roomacoustics, Applied Science, London 1982, Vol. 2, p.20, p.343

/2/ Lord Rayleigh: Theory of Sound, Vol. 2 1878, p.323, 326, McMillan, London

/3/ Cremer, L.: The Physics of the Violin, MIT Press, Cambridge MA, 1984, p.384, p.362

/4/ Backhaus, H.: Naturwissen 17 (1929) 811

/5/ Weinreich, G.: J. Acoust. Soc. Amer. 77 (1985) 710

/6/ Meinel, H.: Akust. Z. 2 (1937) 22

/7/ Cremer, L. Acustica 55 (1984) 44

/8/ Cremer, L. and Wang, M.: Acustica, in press

/9/ Heaviside, O.: Electrical Papers, 1882, Vol. 1, p. 520

/10/ Wagner, K.W. : Einfuhrung in die Lehre von den Schwingungen und Wellen, Dietrich' sche Verlags-handlung, Wiesbaden 1947, p.180

/11/ Wang, M.: Master-Thesis, Technical University Berlin, Oct. 1986

/12/ Morse, P.M. and Ingard, K.U.: Theoretical Acoustics, MacGraw Hill, New York 1968, p. 340

/13/ Akyol, T.P.: Acoustica 61 (1986) p. 200

/14/ Copley, L. G.: J. Acoust. Soc. Amer. 41 (1967) p. 807 and 44 (1968) p. 28

/15/ Fenlon , F.H.: Proc. IEEE 57 (1969) p. 291

/16/ Sandman, B.E.: J. Acoust. Soc. Amer. 60 (1976) p. 1256

/17/ Shenderov, E.L. and Kozyrev, V.A.: Soviet Physics Acoustics 26 (1980) p. 230

/18/ Williams, W., Parke, N. G., Moran, D.A. and Sherman, C.H.: J. Acoust. Soc. Amer. 36 (1964) p. 2316

The author is very indebted to his colleague, Dr. J. Woodhouse, University of Cambridge, for reading and improving his text

	$\frac{\mathrm{Im}\{\int Q_0 \Pi_2^* dS\}}{-4\pi kh^3}$	$\frac{\mathrm{Im}\{\int Q_2 \Pi_0^* dS\}}{-4\pi kh^3}$
plates	$\frac{1}{24}+\frac{1}{24}\left(\frac{h}{a}\right)^4-\frac{1}{12}\left(\frac{h}{a}\right)^6$	$\frac{1}{24}+\frac{3}{8}\left(\frac{h}{a}\right)^4-\frac{5}{12}\left(\frac{h}{a}\right)^6$
zone	$-\frac{1}{6}\left(\frac{h}{a}\right)^4+\frac{1}{6}\left(\frac{h}{a}\right)^6$	$-\frac{1}{2}\left(\frac{h}{a}\right)^4+\frac{1}{2}\left(\frac{h}{a}\right)^6$
sum	$\frac{1}{24}-\frac{1}{8}\left(\frac{h}{a}\right)^4+\frac{1}{12}\left(\frac{h}{a}\right)^6$	$\frac{1}{24}-\frac{1}{8}\left(\frac{h}{a}\right)^4+\frac{1}{12}\left(\frac{h}{a}\right)^6$

Table 1

$$\frac{1}{4\pi h^2 (kh)^2}\int \underline{Q}_m \underline{\Pi}_m^* . dS \quad \text{for} \quad kh = 0.2, \; h/b = 1/4$$

REAL PART OF THE MATRIX COEFFICIENTS:

0.1923E+00	-0.1077E-03	-0.1441E-04	-0.2927E-05
0.1077E-03	0.7867E-06	0.4010E-07	0.1220E-07
0.1441E-04	-0.4010E-07	0.2057E-12	0.1311E-13
0.2928E-05	-0.1220E-07	-0.1311E-13	0.1177E-19

IMAGINARY PART OF THE MATRIX COEFFICIETS:

-0.5102E+00	-0.4128E-01	-0.6205E-02	-0.1100E-02
-0.4128E-01	-0.2094E-01	-0.7831E-02	-0.2608E-02
-0.6205E-02	-0.7831E-02	-0.5477E-02	-0.2932E-02
-0.1100E-02	-0.2608E-02	-0.2932E-02	-0.2304E-02

Table 2

$$\frac{1}{4\pi h^2 (kh)} \int \underline{Q_m \Pi^*_m} dS \quad \text{for} \quad kh = 3.2, \ h/b = 1/4$$

REAL PART OF THE MATRIX COEFFICIENTS:

0.2847E+00	-0.2215E-01	-0.8591E-02	-0.1454E-02
0.2215E-01	0.6470E-01	0.4607E-03	0.3150E-03
0.8591E-02	-0.4607E-03	0.6304E-02	0.3876E-03
0.1454E-02	-0.3150E-03	-0.3876E-03	0.2770E-04

IMAGINARY PART OF THE MATRIX COEFFICIETS:

-0.4721E-01	0.1006E-01	0.2517E-02	0.1252E-03
0.1006E-01	-0.1459E-01	-0.8076E-02	-0.2019E-02
0.2517E-02	-0.8076E-02	-0.9187E-02	-0.4074E-02
0.1252E-03	-0.2019E-02	-0.4074E-02	-0.2875E-02

Table3

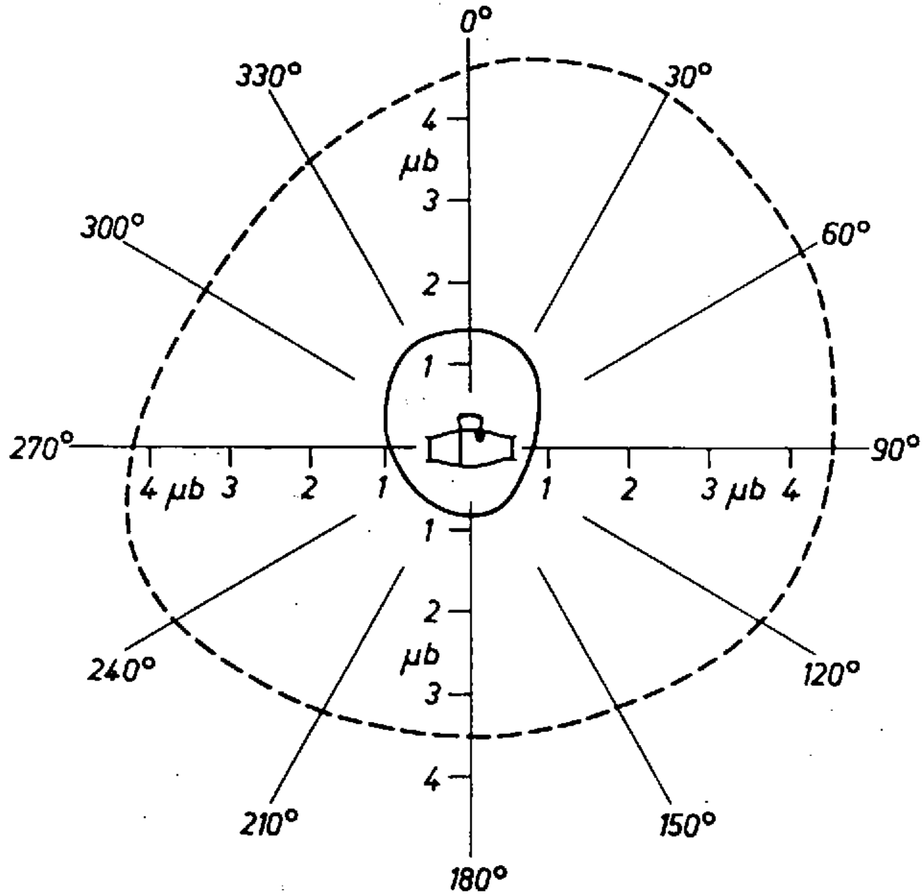

Fig. 1: Measured directional characteristic of a violin in the bridge plane by Meinel (1937). Solid line 290Hz, dashed line 517Hz.

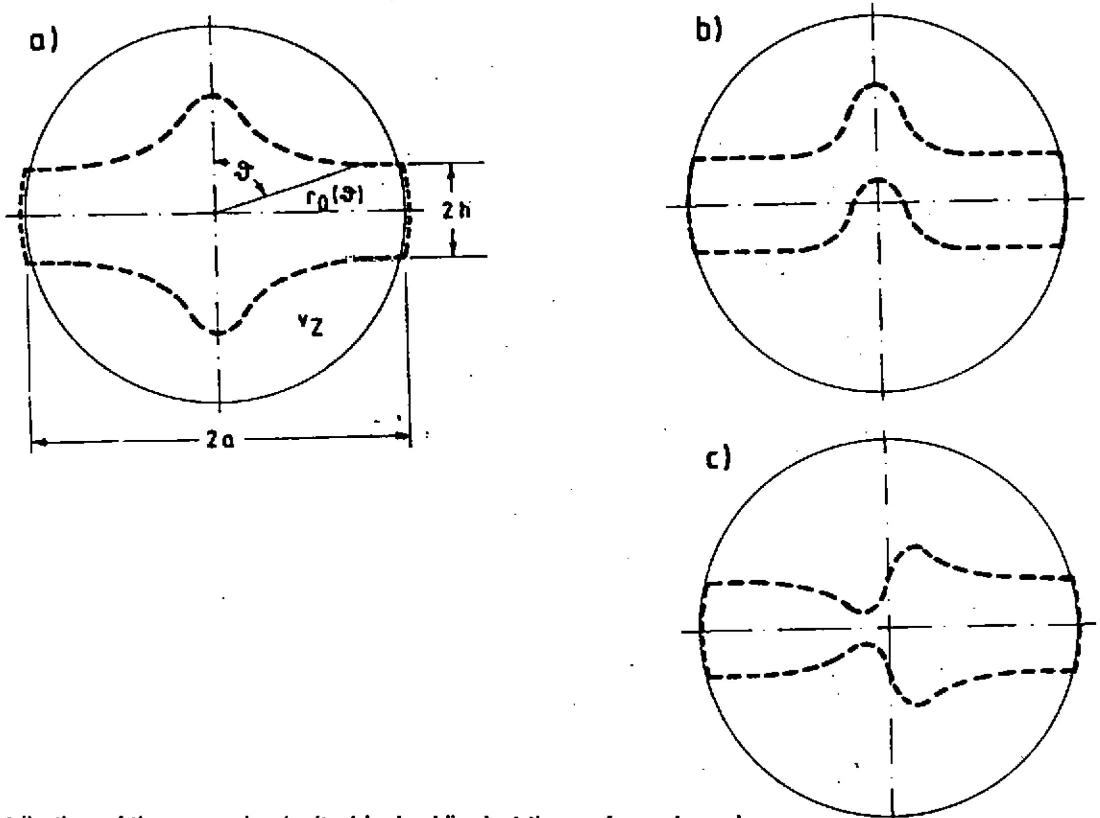

Fig. 2: Distribution of the normal velocity (dashed line) at the surface of a sphere-zone with top- and back-plated

a) for a zero-order spherical field,
b) for a first-order spherical field in z- direction
c) for a first order field in z-direction

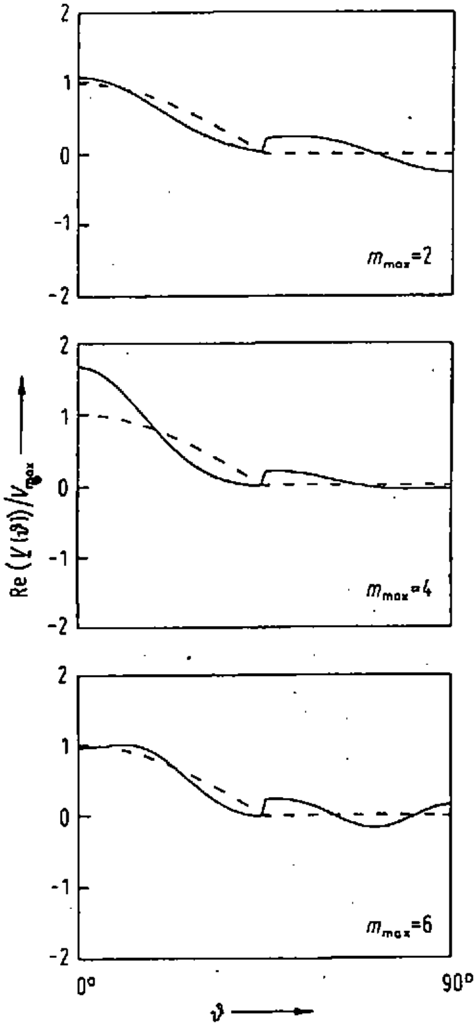

Fig. 3: Approximation of the real part of $\sum \underline{V}_m \underline{Q}_m$ (solid line) V to V(θ) for increasing m_{max} for a cylinder (h/b = 1/1) and a Helmholtz-number (kh = 0,2)

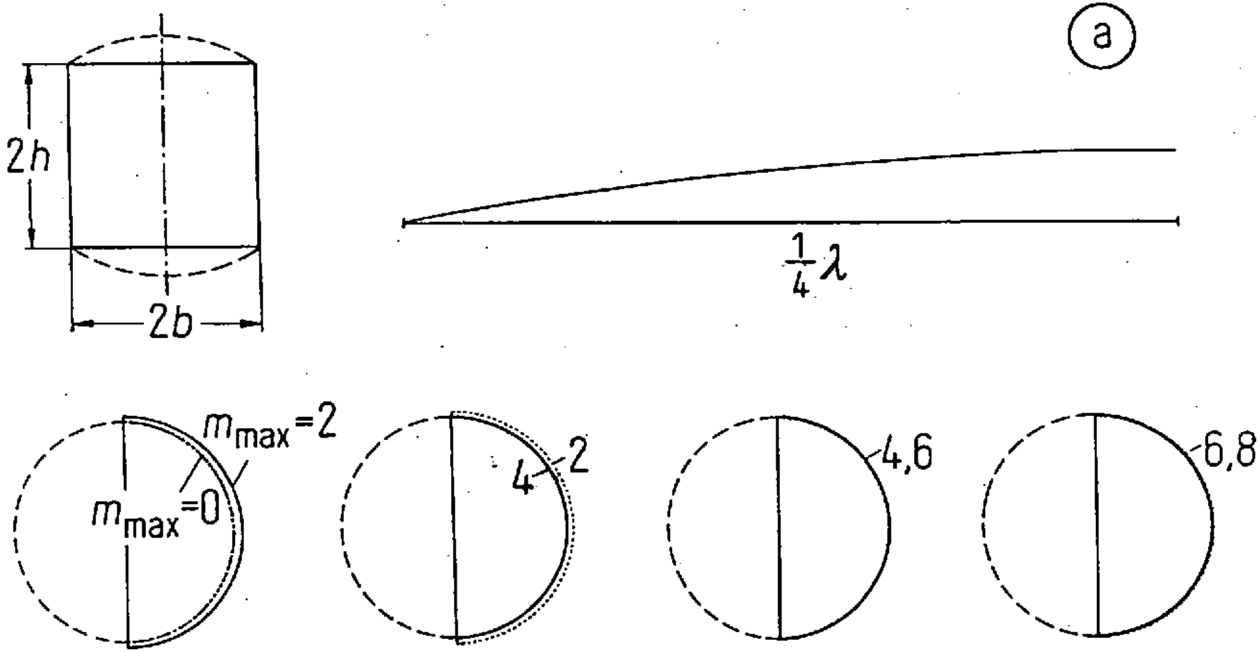

Fig. 4: Directional characteristics $\underline{p}(\theta)$ of a cylinder, above, left, shape: h/b = 1/1, right, wavelength in same scale: kh = 0,2, below characteristics $|\underline{p}(\theta)|$ calculated for growing m_{max}, compared with approximation for zero order (dashed line)

SOUND FIELD SYNTHESIS

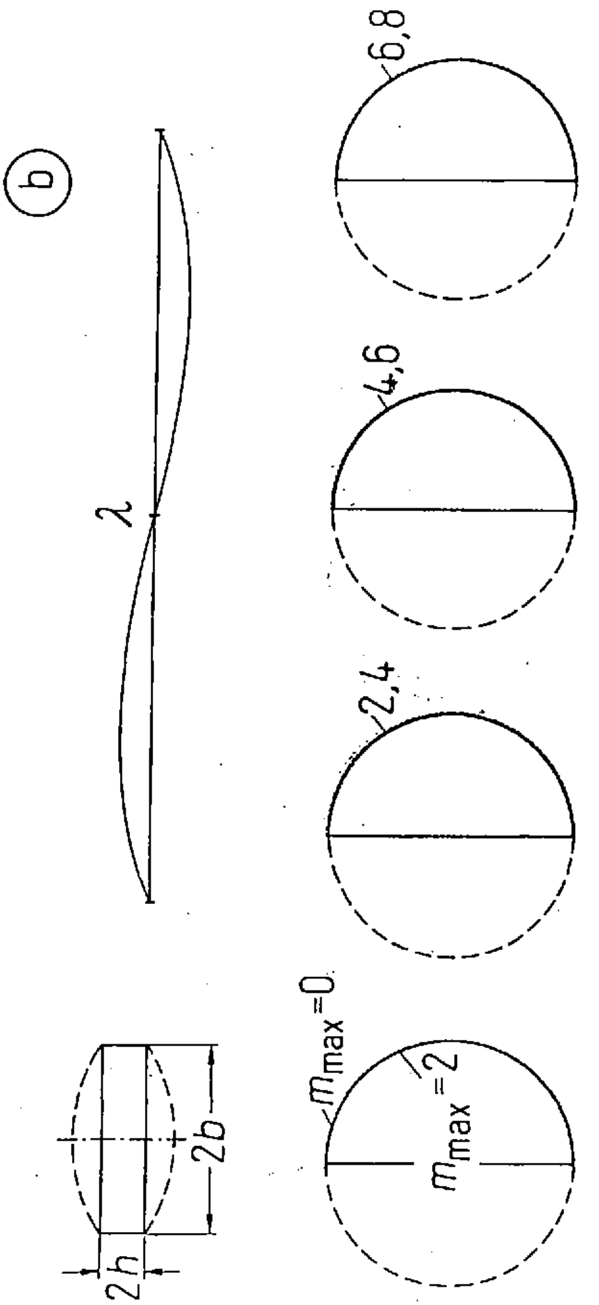

Fig. 5: the same as Fig. 4, but h/b = 1/4

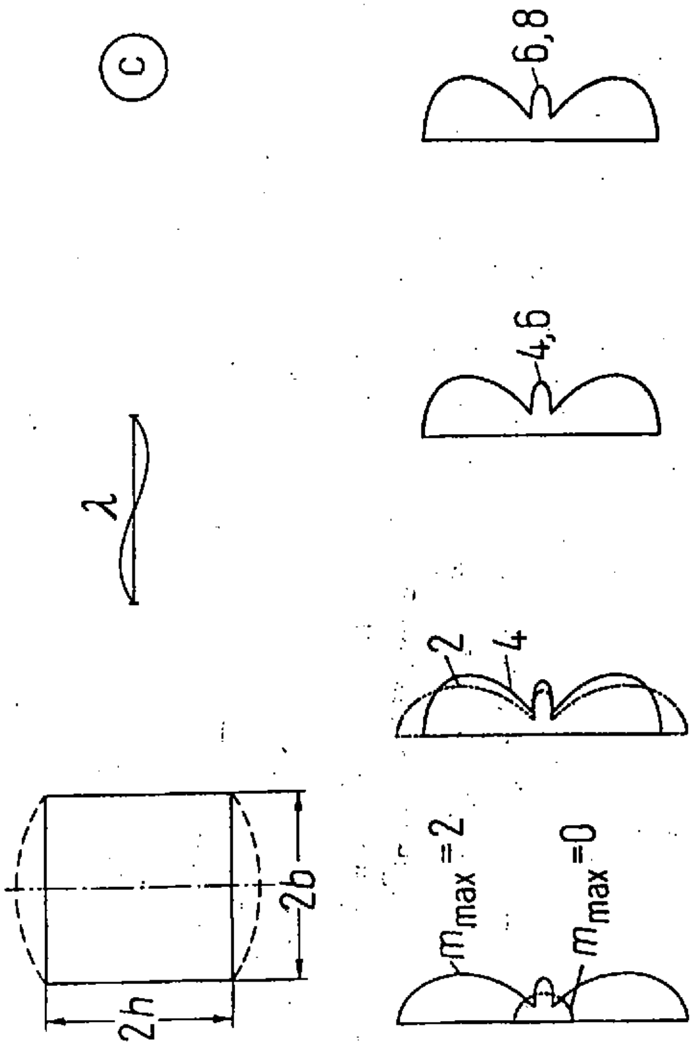

Fig. 6: the same as Fig. 4, but kh = 3,2; without approximation

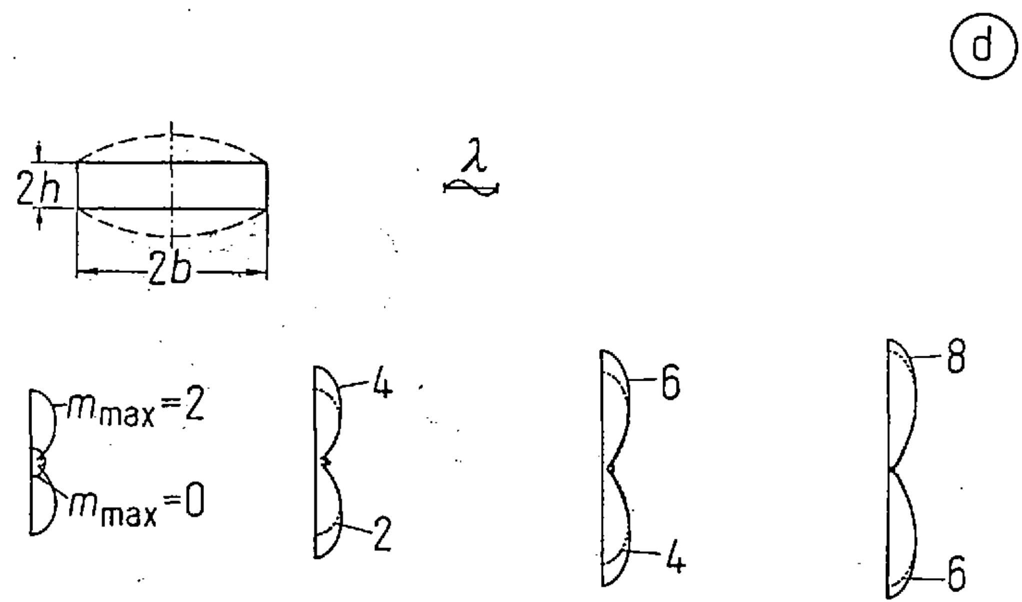

Fig. 7: the same as Fig 4, but h/b = 1/4, kh = 3,2; without approximation

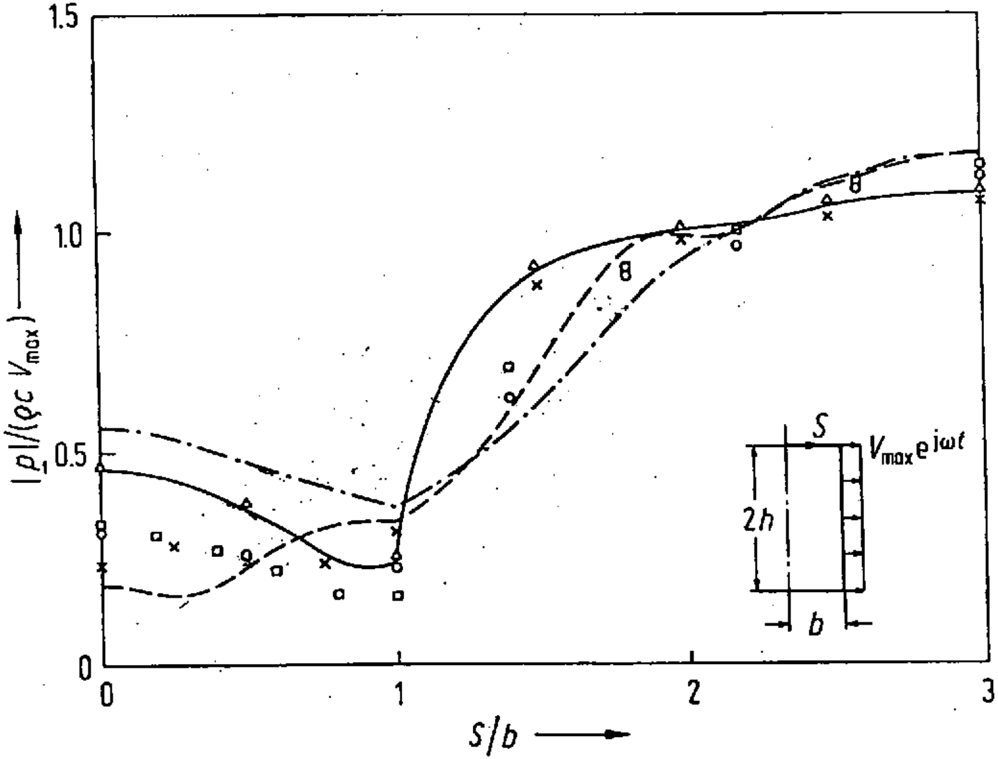

Fig. 8: Comparison of calculated pressure-distributions |p(s)| at the surface of a cylinder (h/b = 2/1), when its shell vibrates with constant velocity and the end-plates are in rest, solid line after Akyol, triangles after Shenderov, circles after Copley, squares after Fenlon, crosses afetr Sandman, dashed line after Cremer/Wang and dashdotted line after Williams et al. - over the distance s from plate-center till shell-middle along the surface.

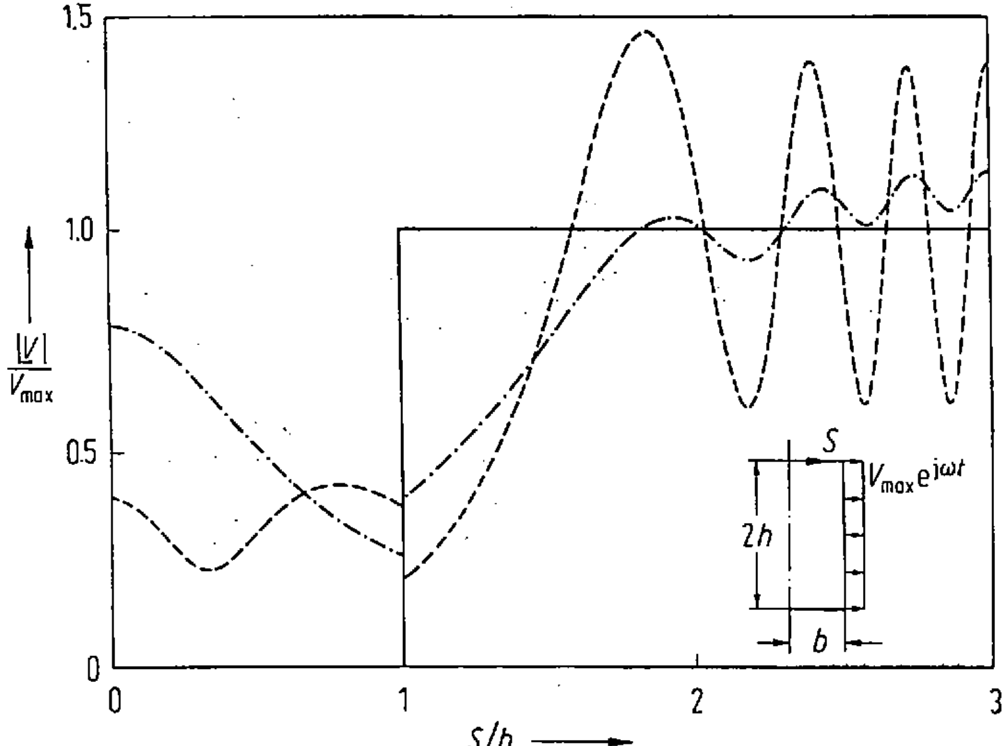

Fig. 9: Distribution of the normal velocity V(s) at the example described in Fig. 8; solid line: given V(s), dashed line: calculated after Cremer-Wang; dashdotted line: calculated after Williams et al.;

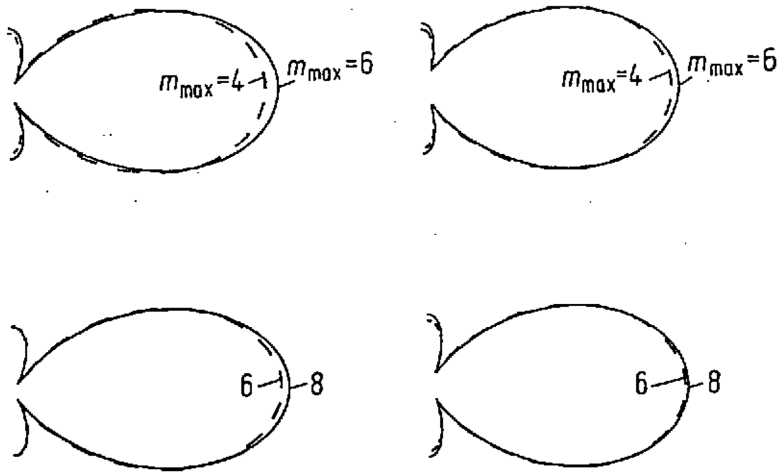

Fig. 10: Calculated directional characteristics $|\underline{p}(\theta)|$ for the example described in Fig. 8; left: according to Williams et al.; right: according to Cremer-Wang.